Research Article

Macroscopic Effect of Small Intestine Submucosa Hydrogel-Silver Nanoparticles Composite on Healing of Infected Wounds

Saddam Hummadi[1], Nadia Al-Falahi[2*]

[1]Department of Surgery and Obstetrics, College of Veterinary Medicine, Tikrit University, Iraq; [2]Department of Surgery and Obstetrics, College of Veterinary Medicine, Baghdad University, Iraq.

Abstract | Treatment of infected wounds is one of the common challenges in veterinary practice. This study highlights the synthesis and use of hydrogel derived from small intestine submucosa (SIS) and AgNPs composite for accelerate the healing of infected wounds and improve cosmetic outcomes. A 5% w/v SIS hydrogel was prepared and formulated with 100 µg/ml AgNPs to evaluate its effect on healing of infected wounds in rabbit. Forty eight adult rabbits aged 8-12 months, weighing 1.5-2.5 kg, were divided randomly into three equal groups (n=16) after inducing infected wounds. In control group (GI), the infected wounds were managed by rinsing with normal saline after debridement and bandaging without any topical application. In SIS hydrogel group (GII), the infected wounds were treated by application of SIS hydrogel after wound management. In SIS hydrogel-AgNPs composite group (GIII), the infected wounds were treated by application of composition of SIS hydrogel and AgNPs after wound management. The wound healing was assessed clinically macroscopically by measurement of wound contraction at days (0, 3, 6, 9, 12, 15, 18, 21, 24, 27 and 30) post treatment in addition to macroscopic finding images (3, 7, 14 and 30 days) post treatment to monitoring the changing in wound bed. Such investigation indicates that the percentage of wounds closure were significantly increased (P≤0.05) in GII and GIII as compared to GI from day six extended to day thirty, while the significant increase in wounds closure in GIII were began from day 15th until day 24th post treatment and completely closed at day 27th without scar formation, in contrast with wounds area of GII which was nearly closed at periods of day 30th, while the wounds of GI exhibited incomplete closure at the same period. In conclusion, the composite bioscaffold integrates the properties of AgNPs with those of SIS hydrogel, providing a synergistic effect for wound healing improvement and showed the best outcome in healing of infected wound.

Keywords | Infected wound, Healing, Small intestine submucosa (SIS), hydrogel, Silver nanoparticles (AgNPs), Topical applications, Rabbits.

Received | October 27, 2023; **Accepted** | November 20, 2023; **Published** | January 05, 2024
***Correspondence** | Nadia Al-Falahi, Department of Surgery and Obstetrics - College of Veterinary Medicine-Baghdad University, Iraq; **Email:** nadia.hvet@covm.uobaghdad.edu.iq
Citation | Hummadi S, Al-Falahi N (2024). Macroscopic effect of small intestine submucosa hydrogel-silver nanoparticles composite on healing of infected wounds. Adv. Anim. Vet. Sci. 12(2): 216-225.
DOI | http://dx.doi.org/10.17582/journal.aavs/2024/12.2.216.225
ISSN (Online) | 2307-8316

INTRODUCTION

Wounds in animals are a common reason for demand veterinary attention (Shi et al., 2020). The way in which wounds are managed affect the rate of healing, the time to return to normal function and the final cosmetic outcomes (Atwan and Hayder, 2020). The management of wound is differing by the use of antiseptics and antimicrobials, adherent and non-adherent dressings, and miscellaneous topical applications (Shi et al., 2020).

Infection is the most common problem associated with wounds healing (Al-Ogaidi et al., 2017). Consequently, effective treatments are necessary to reduce wound bacterial colonization and infection, in order to improve the healing process (Liu et al., 2022).

Small intestinal submucosa (SIS) is a natural biomaterial derived from the small intestine of vertebrates; That consists of collagen, proteoglycan glycosaminoglycan, glycoprotein, and growth factors, all of which together make SIS an excellent choice as an ideally implanted material for tissue engineering and clinical applications (AL-Falahi and Salih, 2016). The benefits of using SIS are two folds; firstly, it provides a scaffold to reconstruct and repair the host tissue, and secondly, it signals the surrounding host cells to grow, to form new vessels, and to foster cellular differentiation, which initiates site specific tissue remodeling Wang et al., (2018). The SIS has a high potential to use as full-thickness wound dressing with the ability to enhance healing of the clean and infected wound with little formation of scar tissue (Al-Falahi, 2009; AL-Bayati et al., 2016).

Hydrogels, the cross-linked polymer networks, are smart enough to respond the fluctuations of environmental stimuli (pH, temperature, ionic strength, electric field, presence of enzyme etc.) (Meleties et al., 2021). In their swollen state, they are soft and rubbery, resembling the living tissue exhibiting excellent biocompatibility through supporting cell proliferation and migration, this feature will maintain a moist environment and thus help to relieve the discomfort of the lesion and reduce the probability of scarring. (Pan et al., 2019).

Antimicrobial activity of nanoparticles being an approach of regenerative medicine (Abd AL-Rhman et al., 2016). Silver nanoparticles (AgNPs) have been shown to be anti-inflammatory (Singh et al., 2022) and have bactericidal properties against *Staphylococcus aureus, Staphylococcus epidermidis, E. coli*, and *P. aeruginosa* (Mohammed et al., 2018; Ali and Khudair, 2019). The current study focuses on synthesis and application of a small intestine submucosa hydrogel-AgNPs composite for treatment of infected wounds in a rabbit model.

MATERIALS AND METHODS

Experimental Animals

Forty eight clinically healthy adult male rabbits, aged (8-12 months), weighing (1.5-2.5 kg) were enrolled in current study. The experimental animals preconditioned in the animal facility for at least 14 days prior to initiation of the study. They were subsequently individually housed in (60 × 50× 50) centimeters metal crates at standard room temperature (22 ± 3C°) throughout the experiment, receiving free accesses to water and food. All experimental animals were dewormed with ivermectin (Intermectin® 1%, Holland) in a dose of 0.2 mg/kg of body weight were injected subcutaneously with intervals of 11 days for 2 times (Kumar et al., 2018). All procedures used in this study were approved by care and use committee No. 915 in 24th April 2022, College of Veterinary Medicine, University of Baghdad during a period extending from 27th December 2020 to 21st October 2021.

Experimental Design

The experimental animals (n=48) were divided randomly into three equal groups (n=16) after inducing infected wounds: in gontrol group (GI) (n=16) the infected wounds were managed by rinsing with normal saline after debridement, and bandaging without any topical application, in SIS hydrogel group (GII) (n=16): the infected wounds were treated by application of small intestine submucosa hydrogel after the previously wound management, and in SIS hydrogel-AgNPs composite group (GIII) (n=16) the infected wounds were treated by application of composition of SIS hydrogel and silver nanoparticles after the previously wound management (Mahmood and Mahdi, 2022).

Wounds in all groups were evaluated macroscopically by measurement of wound contraction at days (0, 3, 6, 9, 12, 15, 18, 21, 24, 27 and 30) post treatment as described by Hummadi, (2015), in addition to macroscopic finding Images (3, 7, 14 and 30 days) post treatment to monitor the changing in wound bed.

Technique Of Induce Infected Wounds

The experimental animals were anesthetized with an intramuscular administration of a mixture of 5mg/kg body weight of xylazine hydrochloride (XYL-M2® 20 mg/ 1ml, Belgium) and 35mg/kg body weight of ketamine hydrochloride (alfason® 10%, Holland) (Oguntoye and Oke, 2015). The back region was prepared for aseptic surgery, then Circular full-thickness skin wound with 2 cm in diameter was created on the dorsal aspect of lateral thoraco-lumber area of animal (Fig.4A), using a cylindrical metal tube with sharp end that was made for this purpose, to define the edges of the wound precisely (Fig.4B). After creation of wounds, 10 µl of the gram positive Methicillin-resistant *Staphylococcus aureus* bacterial isolate at concentration of 1×10^6 Colony-forming unit per milliliter was spread along the created wounds by using insulin syringe. All wounds were left 48 hours to induce infected wounds (Yang et al; 2020) (Fig.4C).

Treatment Of Infected Wounds

All induced infected wounds were cleaned and debrided to remove necrotic and infected tissue (Fig.4D), than were irrigated with a continuous and pulsatile flow of saline solution for several minutes then the previously prepared SIS hydrogel (In second group) and SIS hydrogel-AgNPs composite (In third group) was applied onto the wound defect with syringe needle (gauge 18), the amount of ap-

plied gels ranged from 0.5-1 ml until filled the skin defect and reached the same level of adjacent normal skin edges (Fig.4E and F). The wounds of the three groups of animals were covered with occlusive breathable film (Tegaderm™ ,6 cm x 7 cm, USA by 3M health care) (Fig.4G) (Liu et al., 2022; Firlar et al., 2022)

Preparation Of Small Intestine Submucosa (Sis)

The bovine small intestine was obtained from slaughtering house immediately after sacrifice. Connective tissue and adipose tissue were removed from the serosal surface and any residual ingesta were removed by repeated washes with tap water (White et al., 2016). The small intestine was cut in length of approximately 10 cm and washed with a saline solution (Claudio-Rizo et al., 2016). SIS was obtained by mechanical removal of the tunica serosa, tunica muscularis, and mucosa then cleaned by washing continuously with a saline solution. The submucous membrane was submerged in a solution containing methanol 100 % (Haymankimia®) and chloroform 99.8% (SDFCL, India) (1:1, V/V) for 12 h and rinsed with the deionized water to remove the organic solvents. The membrane was incubated in the 0.05% trypsin (HIMEDIA®, India)/0.05% ethylenediamine tetraacetic acid (SDFCL, India) at 37 °C for 12 h and rinsed with a saline solution continuously to remove the trypsin. Subsequently, the membrane was further treated with 0.5% sodium dodecylsulphate (Alpha Chemika, India) in 0.9% sodium chloride by continuously shaking on an orbital shaker for 4 h. Then, the detergent was removed by thoroughly rinsing with a saline solution. Finally, the submucous membrane was soaked into 0.1% peroxyacetic acid and 20% ethanol (100% chem-Lab, Belgium) for 30 min and rinsed with saline solution. Samples of SIS after decellularization were sectioning and staining with Hematoxylin and Eosin stain, and examined histologically to detect the complete removal of cells. All the samples were frozen-dried under -70 °C overnight with a lyophilizer and sealed into airtight packages (Luo et al., 2011).

Preparation Of Sis Hydrogel And Silver Nanoparticles Composite

The SIS hydrogel was prepared according to Zhao et al. (2021) with modification as follow; The SIS pieces were pulverized, suspended in HCl (Honeywell, Fluka®) solution with pepsin (HIMEDIA®, India) (1 mg/mL pepsin in 0.01 M HCl, 72 hr.), stirred (60 rpm) constantly for 48 hr. at room temperature, adjusted to pH 7.4, lyophilized (-70 °C) and powdered using electrical mill assisted by liquid nitrogen to obtain an SIS powder, sealed into airtight packages and then sterilized by using gamma irradiation (25KGY) and stored at - 20° C. until use. The SIS powder will be dissolved in phosphate-buffered saline (PBS) at 50% w/v (50 mg/ml) and shaped into a gel overnight at 37 °C. The hydrogel can be applied into a specific area with a syringe based on the good fluidity of hydrogel. The Small Intestine Submucosa (SIS) powder was dispersed in PBS at 50% w/v, a characterized AgNPs (Fig.1, 2 and 3) was incorporated within SIS-PBS suspension at concentration of 100 µg/ml (LewisOscar et al., 2021) and incubated overnight at 37 °C to be converted into a gel.

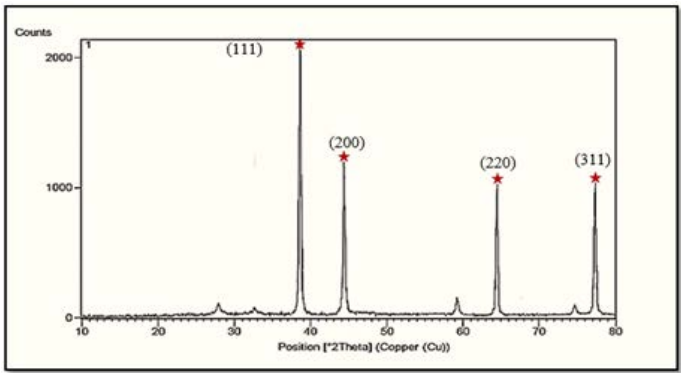

Figure 1: XRD pattern of AgNPs. Shows the diffraction peaks of 38.5, 44.4, 64.55 and 77.32 corresponded to the (111), (200), (220), and (311) planes respectively.

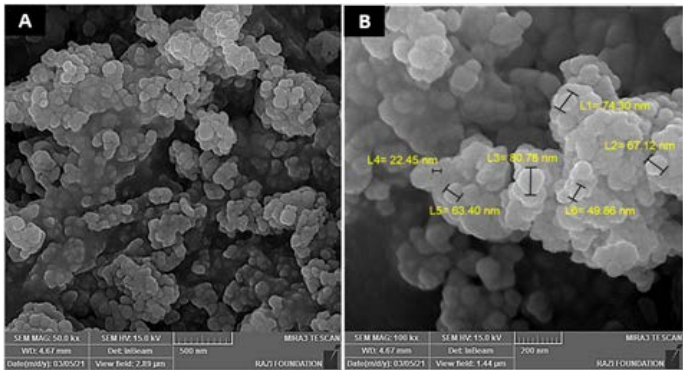

Figure 2: Scanning electron microscope (SEM) images of silver nanoparticles synthesized using Aloe Vera gel extracts at different magnifications. (A) at 50 kx magnifications, shows uniformly spherical shape nanoparticles with smooth edges.(B) at 100 kx magnifications, shows particles size ranged from 22.45 nm to 80.78 nm.

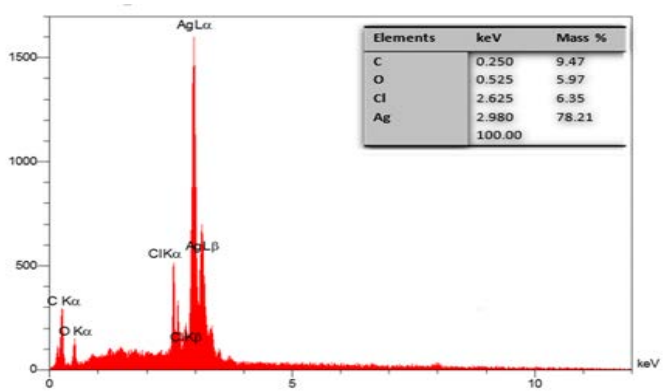

Figure 3: Energy dispersive X-ray (EDX) analysis of silver nanoparticles, shows a strong signal for the Ag atoms, other peaks observed were represent carbon (C), oxygen (O) and chlorine (Cl).

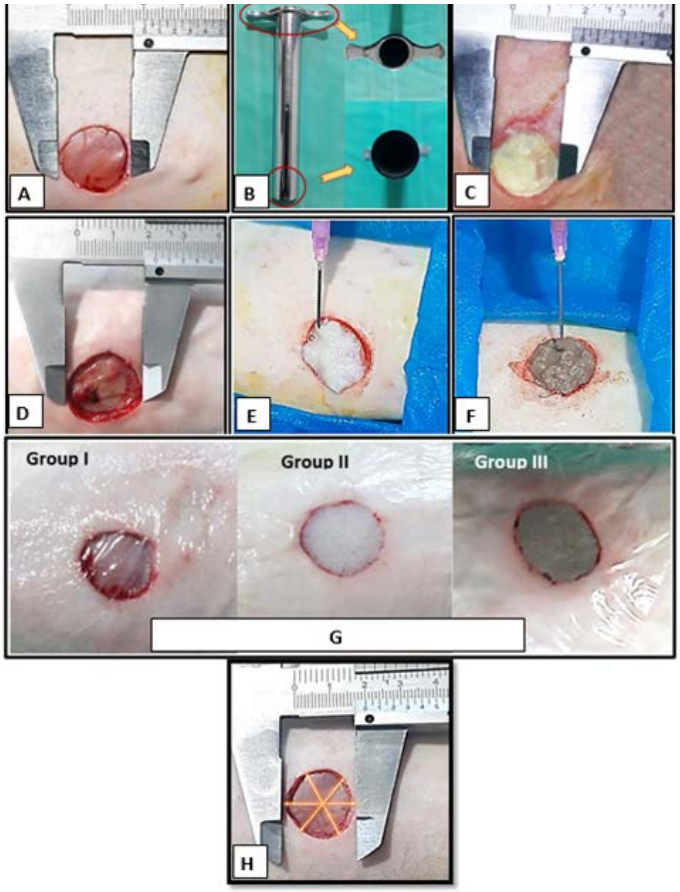

Figure 4: (A) Creation of circular full-thickness skin wound with 2 cm in diameter. (B) Shows a cylindrical metal tube with sharp end used for induce circular wound. (C) The induced infected wound. (D) Shows the infected wound after cleaning and debridement. (E) Application of SIS hydrogel on wound area. (F) Application of SIS hydrogel- AgNPs composite on wound area. (G) Shows covering of the wounds by Tegaderm in GI, GII and GIII. (H) Measurement of three different diameters of wound using a Vernier caliper.

Clinical Evaluation

The general health status of the animals clinically evaluated including body temperature, respiratory and pulse rates was checked once daily after inducing wounds and during treatment and estimate local changing such as signs of inflammation or infection.

Macroscopic Evaluation

The percentage of wound contraction was calculated after measuring three different diameters using Vernier caliper, each one cross another at the center of the wound with equal distance among them (Dunn et al., 2013) (Fig.4H), the average of these three diameters were calculated and inserted in equation, as follows:

Where $\mathbf{A_0}$ was the area of the initial wound, and $\mathbf{A_n}$ was the wound area on the day of assessment (Wei et al., 2019), for each of the time points (days 0, 3, 6, 9, 12, 15, 18, 21, 24, 27 and 30). Furthermore the wounds of all groups were follow-up by digital camera at 3, 7, 14, and 30 days post treatment.

Statistical Analysis

The Statistical Analysis System- SAS program (Cary, 2018) was used to detect the effect of difference factors in study parameters. Least significant difference test (Analysis of Variation-ANOVA) was used to significant compare between means in this study.

RESULTS

Clinical Evaluation

Daily clinical monitored of animals after infected wound creation exhibited systemic signs which including; Pyrexia, tachycardia, tachypnea, anorexia and fatigue. These signs begun clearly after first 24 hours post wounding.

The mean values of physical parameters (body temperature and respiratory) rate were listed in charts (1 and 2). This data evacuated a significant increasing (P≤0.05) in the values of these parameters for animals in all groups particularly at the first three days post inducing infected wound.

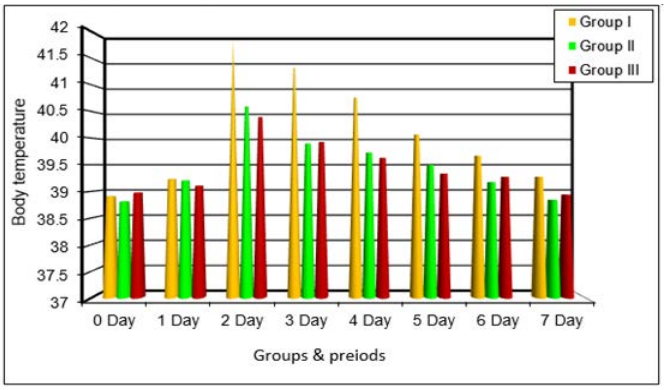

Chart 1: The mean values M± SD of body temperature (Degrees Celsius °C) during the first weak pre and post-induced infected wound and treatment.

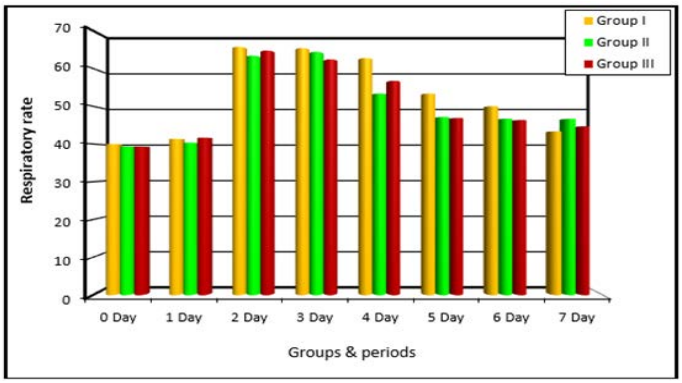

Chart 2: The mean values M± SD of respiratory rate (breaths per minute) during the first weak pre and post-induced infected wound and treatment.

Table 1: Shows the mean values Mean ± SE of wound contraction during the period of the study in all groups.

Period	Mean ± SE of Contraction (%)			LSD value
Days	Group I	Group II	Group III	
0	0.00 ±0.00	0.00 ±0.00	0.00 ±0.00	0.00 NS
3	13.75 ±0.15 **a**	12.17 ±1.39 **a**	12.70 ±2.40 **a**	3.13 NS
6	26.54 ±5.65 **b**	49.53 ±1.88 **a**	59.53 ±2.28 **a**	11.78 *
9	50.32 ±3.23 **b**	67.09 ±1.05 **a**	71.91 ±2.17 **a**	7.453 *
12	57.91 ±2.03 **b**	70.89 ±1.27 **a**	73.26 ±0.96 **a**	4.779 *
15	59.36 ±2.86 **c**	72.68 ±1.28 **b**	82.23 ±0.97 **a**	6.061 *
18	64.10 ±2.94 **c**	77.01 ±2.43 **b**	89.95 ±1.29 **a**	7.452 *
21	68.62 ±2.67 **c**	80.26 ±4.56 **b**	93.27 ±1.36 **a**	10.085 *
24	77.17 ±1.24 **c**	89.87 ±1.65 **b**	98.91 ±0.64 **a**	4.012 *
27	84.39 ±2.31 **b**	96.25 ±1.08 **a**	100 ±0.00 **a**	4.716 *
30	93.15 ±1.67 **b**	99.56 ±0.43 **a**	100 ±0.00 **a**	3.195 *

Means having with the different letters in same row differed significantly. * (P≤0.05), NS: Non-Significant.

In the first group there is a significant increasing (P≤0.05) in body temperature at 2, 3 and 4 days post induced infected wounds (41.87 ±2.06, 41.33 ±2.15, 40.07 ±2.17 and 40.77 ±1.92) respectively, while in the second and third group there is a significant increasing (P≤0.05) at days (2 and 3) post induced infected wound (40.60 ±1.98 and 39.90 ±1.60) and (40.40 ±2.09 and39.93 ±1.37) respectively, and there is a significant increase (P≤0.05) among groups at second, third and fourth day.

The respiratory rate showed a significant increase (P≤0.05) at days (2, 3,4 and 5) in the first group (65.67±4.0, 65.33 ±3.1, 62.67 ±3.8 and53.33 ±3.5) respectively, in the second and third groups, the significant increase (P≤0.05) appeared at days (2, 3 and 4) post inducing infected wound (63.33 ±3.7, 64.33 ±3.9 and 53.33 ±3.1) and (64.67 ±4.2, 62.33 ±3.8 and 56.67 ±3.9) respectively, with a significant increase (P≤0.05) among groups at fourth and fifth day post inducing infected wound.

Additionally, the local signs of infection were appeared gradually after 24 hours post-inducing infected wounds, represented by erythema, swelling with inflammatory exudate and purulent discharge. The most prominent complication post treatment was recurrence of wound infection, that noticed in four rabbits (25%) related to control group (GI), three days post wound management.

Macroscopic Evaluation

Wound Contraction

The wound closure values as well as the microscopic finding are recorded in Table 1. The obtained values of wound areas measurement at three days post treatment showed no significant differences P≤0.05 among control(13.75 ±0.15), SIS hydrogel (12.17 ±1.39) and SIS hydrogel -AgNPs (12.70 ±2.40). The percentage of wounds closure were significantly increased in treated groups P≤0.05 as compared to control group from day six extended to the day thirty post treatment. On the other hand, the values of wound closure percentage in SIS-hydrogel group (GII) shown no significant differences with values of SIS hydrogel -AgNPs composite group (GIII) at 3 day, 6 day, 9 day and 12 day post treatment.

The difference in wound closure percent between (GII) and (GIII) was notice at day 15 post treatment. Precisely, the values related to hydrogel-AgNPs composite group at periods of 15th day (82.23 ±0.97), 18th day (89.95 ±1.29), 21st day (93.27 ±1.36) and 24th day (98.91 ±0.64) were significantly increased P≤0.05 more than that of hydrogel

treated group 72.68 ±1.28, 77.01 ±2.43, 80.26 ±4.56 and 89.87 ±1.65 at the 15th ,18th ,21st and 24th day respectively. Interestingly, the wounds area of hydrogel-AgNPs composite group GIII was completely closed at day 27th post treatment with percent of 100, in contrast with wounds area of hydrogel treated group GII which was nearly closed at periods of day 30th with values of 99.56 ±0.43. The wounds of the control group (GI) exhibited 93.15 ±1.67 closure percent at 30 days post management. In control group (GI) at the 30th day the percent of wound closure (93.15 ±1.67) was significantly decreased P≤0.05 in comparison to wounds of treated groups.

The obtained data evidenced that SIS hydrogel-AgNPs treated group shows the best rate of wounds size reduction comparing with that manifested by SIS hydrogel treated group at periods from 6th to 30th day post treatment.

Macroscopic Finding Images

The wound bed at zero day after debridement of control group (GI) was clearly appeared in contrast with wounds of SIS-hydrogel group (GII) and SIS hydrogel-AgNPs composite group (GIII), which were complete coverage by fresh hydrogels with wound shape adaptability (Fig. 5A, B and C).

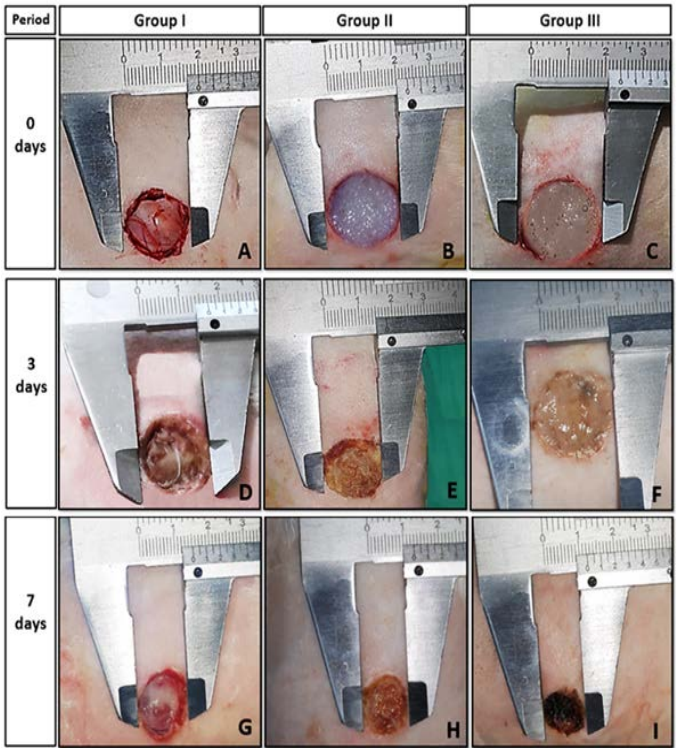

Figure 5: (A) The wound bed at zero day after debridement of group I. (B and C) The wounds of GII and GIII respectively at zero day, which are completely covered by fresh hydrogels. (D) The wound bed of GI at 3rd day shows the beginning of granulation tissue formation with swelling and rounding of wound edges. (E and F) The wounds defect of GII and GIII at 3rd day shows, no clear signs of inflammation, and the hydrogels become more homogenized with increased its adherence to the bed and edges of the wounds. (G) The wounds defect of control group at 7th still unfilled with granulation tissue, with a lesser reduction of wound area compared with GII and GIII. (H and I) The wounds of GII and GIII, respectively at 7th day post-treatment shows the organization and conversion of hydrogels to tissue-like structure.

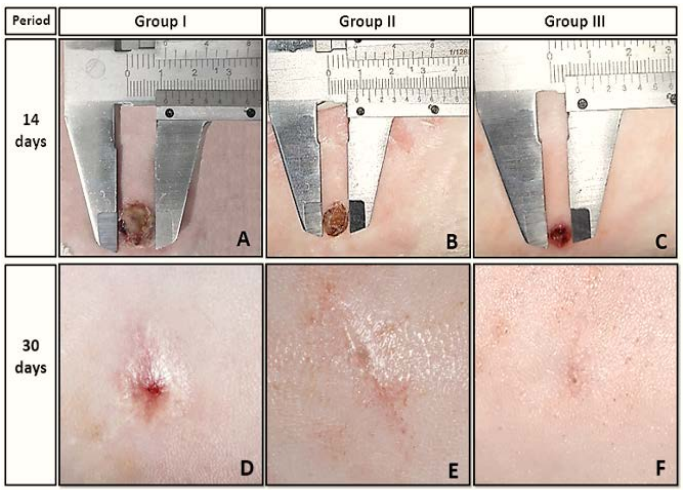

Figure 6: (**A**) The wound bed of GI at 14th day post-management is filled with granulation tissue, which appears higher than the adjacent normal skin. (**B** and **C**) The wounds in GII and GIII respectively at 14th day post treatment, shows the new tissue still at the same level to adjacent normal skin. (**D**) The wounds in GI shows incomplete closure at 30th day post-management. (**E**) The wounds of GII shows complete closure at 30th day post treatment with minimal scar formation. (**F**) The wounds area of GIII at 30th day post treatment disappeared without presence of scar tissue.

At 3rd day post management the wounds bed of GI showed beginning of granulation tissue formation with signs of inflammation such as swelling of wound edges (Lu et al., 2022), (Fig. 5D). At same period the wounds defect of treated groups (GI and GIII) were filled with hydrogels without clear signs of inflammation, as well as the hydrogels become more homogenized with increased its adherence to the bed and edges of the wounds (Fig. 5E and F). At 7th day post treatment the wounds defect of control group (GI) still unfilled with granulation tissue and with lesser reduction of wound area compering with treated groups (Fig. 5G). At the same period in both SIS hydrogel group (GII) and SIS hydrogel-AgNPs composite group (GIII), the hydrogels become organized and converted to tissue like structure with superiority of GIII in term of wound area diminishment (Fig. 5H and I).

At the 14th day post- management in GI the wounds defect filled with granulation tissue covering by dried exu-

dates which appears higher than the adjacent normal skin (Fig. 6A), on the contrary to the wounds of treated groups, the new tissue still at the same level to adjacent normal skin, as well as the wound closure progression was more pronounced in the GIII as compared to the GII and GI respectively (Fig. 6B and C).

Regarding the control group (GI), the wound closure was incomplete at 30th day (Fig. 6D), while the wounds of SIS hydrogel group (GII) were complete closure at 30th day with minimal scar formation (Fig. 6E). Interestingly the wounds area of SIS hydrogel-AgNPs composite group (GIII) were disappeared at 30th day post treatment without presence of scar tissue (Fig. 6F).

DISCUSSION

The present study showed an elevation in body temperature of animals in the control group initially at 2, 3 and 4 days post induced infected wounds, while in treated groups (GII and GIII) an elevation in body temperature occurred at 2nd and 3rd day post induced infected wound with a significant difference (P≤0.05) among control and treated groups at 2nd, 3rd and 4th day. Yang et al. (2020) reported that, the body hyperthermia occurred within 24 hours of bacterial infection and is mediated by the release of endogenous pyrogens such as Interleukins (IL-1 and IL-6). The SIS hydrogel and SIS hydrogel-AgNPs composite were reported to display an anti-inflammatory and antibacterial effects in vitro and in vivo (Singh et al., 2022).

An increasing in respiratory rate in present study correlated with body temperature elevation, this may be due to evoke of body temperature on respiratory rate (Jensen et al., 2019).

In addition to systemic response the infected wound in present study displayed local signs of wounds infection. These signs related to the ability of MRSA to produce the Panton Valentine leukocidin (PVL) toxin that causes lysis of leukocyte as reported by Serra et al. (2015).

The recurrence of wound infection post wound management was noticed in a rate of 25% related to control group in present study. That may attributed to collection of bacteria around the remnants of biofilm within the wound bed followed by recolonization and recurrence of infection. This was supported by Woo, (2016), who suspected that the remnants of biofilm was the primary cause of recurrence of wounds infection.

In the present study the wound closure analysis showed no significant differences among groups at third day post wound treatment. This finding accordance with many studies (Liu et al., 2020), who applied a different types of hydrogel and showed no significant difference of wound closure ratios between control and treated groups in the early stage. That may be ascribed to the time of proliferative phase beginning, in particular, the proliferative phase lasts from around second day of injury to third week (Rodrigues et al., 2019).

Subsequently, from six days extended to the thirty days, the percentage of wounds closure were significantly increased in treated groups as compared to control group. This finding agree with the results obtained by Ma et al. (2022), who investigated the effect of modified SIS hydrogel on full thickness wound in rat model, they found the significantly reduced to the wound areas of treated group on day 7 of treatment compared to the control group. Fujii and Tanaka (2022), indicated that the activated neutrophils are existent after the first 72 h in infected wounds due to tissue trauma caused by bacterial overgrowth or infection that leads elevated the levels of matrix metalloproteinase (MMP), which may be a reason for extensive damage to the extracellular matrix (ECM) and disrupt cell proliferation and migration,

The obtained data in the present study evidenced that GIII shows the best rate of wounds size reduction comparing with that manifested by GII particularly at period from 6th to 30th day post treatment. That indicate the composite bioscaffold integrate the properties of AgNPs with those of SIS hydrogel and providing a synergistic effect for wound healing improvement. The current results were in accordance with Kalirajan and Palanisamy, (2020), who incorporated of AgNPs in collagen hydrogel to treat an open infected wound in rat model, they noticed 100% of wound closure at 24th day of silver nanocomposite tethered collagen scaffold group whereas pristine collagen scaffold treated animals group reveal only 61% of wound closure after 24 days of treatment.

The macroscopic observation of wound bed of control group (GI) in the present study at 3rd day post management showed the signs of unhealthy wound bed which discriminative the degree of inflammatory response tissue trauma or remnant of previous infection. This some extent agree to the Grey et al. (2006), who reported that the dark red colour granulation tissue is the sign of unhealthy new tissue formation, and covering the wounds bed by cream or yellow shiny fibrinous tissue may indicate presence of infection and impedes healing.

In contrast at the same period in present study the wound bed in treated groups completely covered with hydrogels but the margins of the wound appeared without clear signs of inflammation, this finding may explain the efficacy of

hydrogel to enables farther effective debridement in addition to anti-inflammatory and antimicrobial properties of SIS hydrogel and SIS-AgNP composite hydrogel. This interpretation corroborated by Cui et al. (2020) who indicated that the hydrogel donate moisture to the wound, thereby enhancing autolytic removal of foreign material and necrotic tissue.

At 7th day post treatment the wound bed in control group was bright red and partially covered with little amount of pus, indicating that the wound undergoing inflammation and still unfilled with granulation tissue. Same result recorded by Ming et al. (2021), who examined the activity of hydrogel scaffold for accelerates healing of infected wounds, indicating that the uncontrolled serious inflammation due to absence of anti-inflammatory and antibacterial activity in control group.

The macroscopic finding of wounds in treated groups (GII and GIII) at 7th day post treatment, showed the integration between the hydrogels and wounds site. This finding indicate that the hydrogels induced the attachment, growth and organization of the cells and ultimately promoting development of a required tissue. This hypothesis is consistent with many studies which evaluated the efficacy of hydrogels in tissue repair such as Firlar et al. (2022). Fujii and Tanaka, (2022) revealed that the SIS hydrogel providing growth factors assisting wound healing.

In present study the wounds in GI at the 14th day post-management were filled with granulation tissue and dried scab of exudate covered the bed of wound, coincided with a low rate of wound closure compering to treated groups. This finding may be due to impaired wound healing by effect of infection. Studies by Qiu et al. (2020), reported that the presence of wound exudate weakens the defense barrier and stimulate bacterial invasion, prolonged the inflammatory phase, and eventually delayed wound healing.

The grossly finding of wound in GII in current study showed healing without complication and more pronounced wound closure than those in GI, that may reflect the effect of unique properties of SIS hydrogel. This interpretation corroborated by Londono and Badylak, (2015), who reported that SIS hydrogel had more positive effects on matrix gene expressions and cell proliferation. That may explain the minimal scar formation of wounds in SIS hydrogel group in present study at 30th day.

On the other hand, the superiority of GIII in term of wound area diminishment may attributed to coupling of SIS hydrogel with AgNPs SIS lead to optimizing wound healing. In the same line, the study by Tyavambiza et al. (2022), showed that the AgNPs promote the growth of fibroblasts and keratinocytes. In addition to the reduction of the inflammatory cytokines release prevent wound deterioration, AgNPs might improve granulation tissue formation and wound healing (Salem et al., 2022). The results of previous studies revealed to prohealing properties of the AgNP which improved SIS hydrogel, that may explain the disappearing the wound area of SIS hydrogel-AgNPs at 27th day post treatment without scar formation.

CONCLUSIONS AND RECOMMENDATIONS

According to the obtained results, the present study concluded that the bovine small intestine submucosa (SIS) hydrogel-AgNPs composite can be accelerate closure of full thickness infected wound without scar formation in comparing with SIS hydrogel alone. These findings may be due to synergistic effect of SIS hydrogel with AgNPs. More investigations are recommended for detracting the effectiveness of SIS hydrogel in repairing other different types of tissue, such as nerves, tendons, or bones, as well as using other types of metal nanoparticles, such as copper nanoparticles or gold nanoparticles, to detect the most effective one on tissue repair when combined with the SIS hydrogel. As well as fabricating a nanopolymer of SIS hydrogel and studying its effectiveness in healing of infected wounds.

ACKNOWLEDGEMENTS

The authors would like to thank the staff of surgery department, college of veterinary medicine, university of Baghdad for their help in this work.

CONFLICT OF INTEREST

The article was worked and written by the authors and they declare no conflict of interest.

NOVELTY STATEMENT

The novelty of the present study based on the first preparation and local application of small intestine hydrogel – silver nanoparticles composite for treatment of infected wounds, with the aim of investigating the ability of this composite for repair or regeneration of the injured tissues.

AUTHORS CONTRIBUTION

This manuscript has been fulfilled by Synergistic contribution of authors.

DATA AVAILABILITY

Authors will provide all data at the reasonable request.

REFERENCES

Abd AL-Rhman RM, Ibraheem SR, Israa AO (2016). The effect of silver nanoparticles on cellular and humoral immunity of mice in vivo and in vitro. Iraqi J. Biotechnol., 15(2).

AL-Bayati AH, AL-Tememe HA, AL-Mudallal NH. (2016) Role of acellular bovine urinary bladder submucosa on skin wound healing in Iraqi goats. Iraqi J. Vet. Med., 40(1):53-60. https://doi.org/10.30539/iraqijvm.v40i1.138

Al-Falahi N H (2009). Comparative Study for Using of Submucosa of Small Intestine in Healing of Clean and Infected Avulsion Wounds. Iraqi J. Vet. Med., 33 (1): 89-97. https://doi.org/10.30539/iraqijvm.v33i1.720

AL-Falahi NH, Salih SI (2016). A comparative histopathological study of repaired tendons wrapped with two biological matrices in bucks. Adv. Anim. Vet. Sci., 4(3):145-52. https://doi.org/10.14737/journal.aavs/2016/4.3.145.152

Ali ZS, Khudair KK (2019). Synthesis, Characterization of Silver Nanoparticles Using Nigella Sativa Seeds and Study Their Effects on the Serum Lipid Profile and DNA Damage on the Rats' Blood Treated with Hydrogen Peroxide. Iraqi J. Vet. Med., 43(2):23-37. https://doi.org/10.30539/iraqijvm.v43i2.526

Al-Ogaidi I, Salman MI, Mohammad FI, Aguilar Z, Al-Ogaidi M, Hadi YA, (2017). Antibacterial and cytotoxicity of silver nanoparticles synthesized in green and black tea. World J. Experimen. Biosci. 5(1):39-45.

Atwan QS, Hayder NH (2020). Eco-friendly synthesis of Silver nanoparticles by using green method: Improved interaction and application in vitro and in vivo. Iraqi J. Agricult. Sci., 51:201-216. https://doi.org/10.36103/ijas.v51iSpecial.898

Cary N (2018). Statistical analysis system, User's guide. Statistical. Version 9.1th ed., SAS. Institute Inc. USA.

Claudio-Rizo JA, Mendoza-Novelo B, Delgado J, Castellano LE, Mata-Mata JL (2016). A new method for the preparation of biomedical hydrogels comprised of extracellular matrix and oligourethanes. Biomed. Mater., 11(3):035016. https://doi.org/10.1088/1748-6041/11/3/035016

Cui L, Hu J J, Wang W, Yan C, Guo Y, Tu C (2020). Smart pH response flexible sensor based on calcium alginate fibers incorporated with natural dye for wound healing monitoring. Cellulose., 27: 6367-6381 https://doi.org/10.1007/s10570-020-03219-1

Dunn L, Prosser HC, Tan JT, Vanags LZ, Ng MK, Bursill CA (2013). Murine model of wound healing. J. Visualized Exper., 28(75):e50265. https://doi.org/10.3791/50265

Firlar I, Altunbek M, McCarthy C, Ramalingam M, Camci-Unal G (2022). Functional Hydrogels for Treatment of Chronic Wounds. Gels (Basel, Switzerland), 8(2): 127. https://doi.org/10.3390/gels8020127

Fujii M, Tanaka R (2022). Porcine Small Intestinal Submucosa Alters the Biochemical Properties of Wound Healing: A Narrative Review. Biomedicines., 10(9):2213. https://doi.org/10.3390/biomedicines10092213

Grey J E, Enoch S, Harding K G (2006). Wound assessment. Brit. Med. J. (Clinical research ed.), 332(7536): 285–288 https://doi.org/10.1136/bmj.332.7536.285.

Hummadi SK. (2015) Comparative Study between Effect of Punica granatum L. Peel Aqueous Extract and Effect of Honey on Healing of Infected Wound. Tikrit J. Agricult. Sci., 15(3):1-13.

Jensen M M, Kellett J G, Hallas P, Brabrand M. (2019). Fever increases heart rate and respiratory rate; a prospective observational study of acutely admitted medical patients. Acute Med., 18(3): 141–143. https://doi.org/10.52964/AMJA.0766

Kalirajan C, Palanisamy T (2020). Bioengineered Hybrid Collagen Scaffold Tethered with Silver-Catechin Nanocomposite Modulates Angiogenesis and TGF-β Toward Scarless Healing in Chronic Deep Second Degree Infected Burns. Adv. Healthcare Mat., 9(12): e2000247. https://doi.org/10.1002/adhm.202000247

Kumar M, Nath A, Debbarma S, Bhattacharjee S, Monsang S, Bijwal D (2018). Comparative curative efficacy of ivermectin and ivermectin with vitamin supplementation treatment against naturally infested Sarcoptes scabiei Mite in rabbits: a retrospective study. Int. J. Livest. Res., 8(12):82-6. https://doi.org/10.5455/ijlr.20180615034851

LewisOscar F, Nithya C, Vismaya S, Arunkumar M, Pugazhendhi A, Nguyen-Tri P (2021). In vitro analysis of green fabricated silver nanoparticles (AgNPs) against *Pseudomonas aeruginosa* PA14 biofilm formation, their application on urinary catheter. Progress in Organic Coatings, 151:106058 https://doi.org/10.1016/j.porgcoat.2020.106058.

Liu S, Zhang Q, Yu J, Shao N, Lu H, Guo J (2020). Absorbable thioether grafted hyaluronic acid nanofibrous hydrogel for synergistic modulation of inflammation microenvironment to accelerate chronic diabetic wound healing. Adv. Healthcare Mat., 9(11):2000198. https://doi.org/10.1002/adhm.202000198

Liu YF, Ni PW, Huang Y, Xie T (2022). Therapeutic strategies for chronic wound infection. Chinese J. Traumatol. 25(1):11-16. https://doi.org/10.1016/j.cjtee.2021.07.004

Londono R, Badylak S F (2015). Biologic scaffolds for regenerative medicine: mechanisms of in vivo remodeling. Ann. Biomed. Engineer., 43: 577-592. https://doi.org/10.1007/s10439-014-1103-8

Lu Y, Zhao M, Peng Y, He S, Zhu X, Hu C (2022). A physicochemical double-cross-linked gelatin hydrogel with enhanced antibacterial and anti-inflammatory capabilities for improving wound healing. J. Nanobiotechnol., 20(1): 426. https://doi.org/10.1186/s12951-022-01634-z

Luo JC, Chen W, Chen XH, Qin TW, Huang YC, Xie HQ (2011). A multi-step method for preparation of porcine small intestinal submucosa (SIS). Biomaterials., 32(3):706-13. https://doi.org/10.1016/j.biomaterials.2010.09.017

Ma S, Hu H, Wu J, Li X, Ma X. Zhao Z (2022). Functional extracellular matrix hydrogel modified with MSC-derived small extracellular vesicles for chronic wound healing. Cell Proliferation., 55(4): e13196. https://doi.org/10.1111/cpr.13196

Mahmood MM, Mahdi AK (2022). Experimental study of the effect of Plantago major leaves extract on contaminated excisional wound healing in rabbits. Iraqi J. Vet. Sci., 36(I):31-9. https://doi.org/10.33899/ijvs.2022.134991.2432

Meleties M, Katyal P, Lin B, Britton D, Montclare J K. (2021). Self-assembly of stimuli-responsive coiled-coil fibrous hydrogels. Soft Matter, 17(26): 6470-6476. https://doi.org/10.1039/D1SM00780G

Ming Z, Han L, Bao M, Zhu H, Qiang S, Xue S (2021). Living bacterial hydrogels for accelerated infected wound

healing. Adv. Sci., 8(24):2102545. https://doi.org/10.1002/advs.202102545

Mohammed HA, Ali MA, Alnasari MS, Al-Hadban W (2018). Application of Randomly Amplified Polymorphic DNA (RAPD) Technique to estimate genetic distance among some methicillin resistant *Staphylococcus aureus* isolated from different Iraqi hospitals. Baghdad Sci. J., 15(4):381-6. https://doi.org/10.21123/bsj.15.4.381-386

Oguntoye CO, Oke BO (2015). A comparison of xylazine/ketamine, diazepam/ketamine and acepromazine/ketamine anaesthesia in rabbit. Sokoto J. Vet. Sci., 12(3):21-5. https://doi.org/10.4314/sokjvs.v12i3.4

Pan H, Fan D, Duan Z, Zhu C, Fu R, Li X (2019). Non-stick hemostasis hydrogels as dressings with bacterial barrier activity for cutaneous wound healing. Mat. Sci. Engineer. C., 105:110118. https://doi.org/10.1016/j.msec.2019.110118

Qiu Y, Wang Q, Chen Y, Xia S, Huang W, Wei Q (2020). A Novel Multilayer Composite Membrane for Wound Healing in Mice Skin Defect Model. Polymers, 12(3):573. https://doi.org/10.3390/polym12030573

Rodrigues M, Kosaric N, Bonham C A, Gurtner G C (2019). Wound healing: a cellular perspective. Physiolog. Rev. 99(1): 665-706. https://doi.org/10.1152/physrev.00067.2017

Salem H F, Nafady M M, Ewees M G E D, Hassan H, Khallaf R A (2022). Rosuvastatin calcium-based novel nanocubic vesicles capped with silver nanoparticles-loaded hydrogel for wound healing management: Optimization employing Box–Behnken design: In vitro and in vivo assessment. J. Liposome Res., 32(1): 45-61. https://doi.org/10.1080/08982104.2020.1867166

Serra R, Grande R, Butrico L, Rossi A, Settimio UF, Caroleo B (2015). Chronic wound infections: the role of *Pseudomonas aeruginosa* and *Staphylococcus aureus*. Expert Rev. Anti Infect. Ther. ;13(5):605-13. https://doi.org/10.1586/14787210.2015.1023291

Shi C, Wang C, Liu H, Li Q, Li R, Zhang Y (2020). Selection of appropriate wound dressing for various wounds. Frontiers Bioengineer. Biotechnol. 8:182. https://doi.org/10.3389/fbioe.2020.00182

Singh H, Purohit S D, Bhaskar R, Yadav I, Bhushan S, Gupta M K (2022). Curcumin in decellularized goat small intestine submucosa for wound healing and skin tissue engineering. J. Biomed. Mat. Res. Part B: Appl. Biomat., 110(1): 210-219. https://doi.org/10.1002/jbm.b.34903

Tyavambiza C, Meyer M, Wusu AD, Madiehe AM, Meyer S. (2022). The Antioxidant and In Vitro Wound Healing Activity of Cotyledon orbiculata Aqueous Extract and the Synthesized Biogenic Silver Nanoparticles. International J. Molecul. Sci., 23(24):16094. https://doi.org/10.3390/ijms232416094

Wang L, Wang W, Liao J, Wang F, Jiang J, Cao C (2018). Novel bilayer wound dressing composed of SIS membrane with SIS cryogel enhanced wound healing process. Mat. Sci. Engineer. C., 85:162-9. https://doi.org/10.1016/j.msec.2017.11.024

Wei Q, Zhang Z, Luo J, Kong J, Ding Y, Chen Y (2019). Insulin treatment enhances pseudomonas aeruginosa biofilm formation by increasing intracellular cyclic di-GMP levels, leading to chronic wound infection and delayed wound healing. America J. Translat. Res., 11(6): 3261–3279.

White L, Keane TJ, Smoulders A, Zhang L, Castleton A, Badylak S (2016). The effects of terminal sterilization upon the biological activity and stiffness of extracellular matrix hydrogels. Front. Bioeng. Biotech: 4. https://doi.org/10.3389/conf.FBIOE.2016.01.00032

Woo K Y. (2016). Physicians' knowledge and attitudes in the management of wound infection. Int. Wound J., 13(5), 600–604. https://doi.org/10.1111/iwj.12290

Yang WT, Ke CY, Wu WT, Tseng YH (2020). Antimicrobial and anti-inflammatory potential of Angelica dahurica and Rheum officinale extract accelerates wound healing in *Staphylococcus aureus*-infected wounds. Scient. Rep.10(1):5596. 5596. https://doi.org/10.1038/s41598-020-62581-z

Zhao LM, Gong M, Wang R, Yuan QJ, Zhang Y, Pi JK (2021). Accelerating ESD-induced gastric ulcer healing using a pH-responsive polyurethane/small intestinal submucosa hydrogel delivered by endoscopic catheter. Regenerat. Biomat., 8(1):rbaa056. https://doi.org/10.1093/rb/rbaa056